Magnetic structure of the triangular antiferromagnet RbFe(MoO_{4})_{2} weakly doped with nonmagnetic K^{+} ions studied by NMR

Yu. A. Sakhratov, M. Prinz-Zwick, D. Wilson, N. Büttgen, A. Ya. Shapiro, L. E. Svistov, and A. P. Reyes

Phys. Rev. B **99**, 024419 — Published 18 January 2019

DOI: 10.1103/PhysRevB.99.024419

Magnetic structure of the triangular antiferromagnet $RbFe(MoO_4)_2$ weakly doped with nonmagnetic K^+ ions studied by NMR

Yu. A. Sakhratov,[1,2] M. Prinz-Zwick,[3] D. Wilson,[1] N. Büttgen,[3] A. Ya. Shapiro,[4] L. E. Svistov,[5,*] and A. P. Reyes[1]

[1] *National High Magnetic Field Laboratory, Tallahassee, Florida 32310, USA*
[2] *Kazan State Power Engineering University, 420066 Kazan, Russia*
[3] *Center for Electronic Correlations and Magnetism EKM, Experimentalphysik V, Universität Augsburg, D86135 Augsburg, Germany*
[4] *A.V. Shubnikov Institute of Crystallography RAS, 119333 Moscow, Russia*
[5] *P.L. Kapitza Institute for Physical Problems, RAS, Moscow 119334, Russia*

(Dated: December 28, 2018)

The magnetic structure of the quasi-two-dimensional antiferromagnet $Rb_{1-x}K_xFe(MoO_4)_2$ with weakly distorted triangular lattice was studied with ^{87}Rb NMR. The samples with $0 \le x \le 0.15$ were studied in the field region near $H_{sat}/3$, where quantum and thermal fluctuations play a decisive role in the formation of the magnetic structure of undoped frustrated triangular $RbFe(MoO_4)_2$. Line-shape analysis reveals that in samples with $x = 0, 0.025$, and 0.075 the magnetic structure is stabilized by the thermal fluctuations, whereas in the sample with $x = 0.15$ the magnetic structure with short-range order within each individual triangular plane and interplanar disorder is realised. The short-range static correlations in this two-dimensional ordered state are in agreement with a theoretical prediction for the XY triangular-lattice antiferromagnet with nonmagnetic impurities by V. S. Maryasin and M. E. Zhitomirsky [Phys. Rev. Lett. **111**, 247201 (2013)].

PACS numbers: 75.50.Ee, 76.60.-k, 75.10.Jm, 75.10.Pq

I. INTRODUCTION

$RbFe(MoO_4)_2$ is an example of a quasi-two-dimensional (quasi-2D) antiferromagnet ($S = 5/2$) with regular triangular lattice structure. In this compound the Fe interplanar exchange interaction J' is approximately a hundred times smaller than the dominant in-plane interaction J ($J'/J \approx 0.01$). The sufficiently strong single-ion hard-axis anisotropy along the threefold axis C^3 governs the coincidence of the main features of $RbFe(MoO_4)_2$ $H - T$ phase diagram[1–6] with the model phase diagram of the XY 2D triangular lattice antiferromagnet (TLAF) studied in detail in Refs. [7–9].

In the low field range, the so-called Y phase is expected on the basis of the XY-model TLAF with an in-plane external field. In a field range near one third of the saturation field ($H_{sat}/3$) a collinear magnetic structure named up-up-down (*uud*) phase is realized. In this field range the field dependence of the magnetization, $M(H)$, becomes flat. At higher fields, $H_{sat}/3 \lesssim H < H_{sat}$, a canted phase known as V phase with two out of three co-directed magnetic sublattices is expected. The directions of the magnetic moments of three sublattices of these phases are shown in Fig. 1(a). The energy preference of such phases out of the plethora of phases with nearly the same magnetic energy can be determined by considering a contribution from thermal and quantum fluctuations to the particular energy. This contribution can be described as an additional biquadratic term with components of two neighboring spins $A(\mathbf{S}_i\mathbf{S}_j)^2$, where A is negative.[10,11] Such interaction makes those phases more likely, where neighboring spins exhibit an almost collinear arrangement with respect to each other. An impressive feature resulting from the fluctuations is the presence of a broad field region where the *uud* phase is established. The realization of this phase is accompanied by a specific plateau on the magnetisation curve at one third of the saturated value ($M_{sat}/3$).

The energy gain for the phases stabilized by fluctuations is small. Because of this in the real 3D TLAF the established magnetic structure is usually defined by other interactions, such as additional in-plane or interplanar interactions of exchange or relativistic nature. $RbFe(MoO_4)_2$ is an excellent example of a quasi-2D TLAF with magnetic structures controlled by fluctuations. The phase boundaries between paramagnetic and ordered phases and the $H - T$ region where the *uud* phase is realized are in quantitative agreement with the phase diagram of the XY model with an in-plane external field.[8] The magnetic phases in the intermediate field ranges are in agreement with the 2D XY model, whereas the low and high field magnetic phases differ from the model.[1,4,5] This fact demonstrates that other interactions define the magnetic structure at those fields.

Here we report a NMR study of the magnetic structure of potassium-doped $RbFe(MoO_4)_2$ in the field region where the *uud* phase is expected, i.e. at the fields near $H_{sat}/3$. This work was inspired by two recent reports. In the first report (Ref. [10]), the properties of the 2D TLAF with XY-anisotropy and random deviation of the exchange interactions of nearest spins were considered theoretically. It was shown, that the contribution to the magnetic energy stipulated by static fluctuations of exchange integrals can be phenomenologically described by the biquadratic term $A'(\mathbf{S}_i\mathbf{S}_j)^2$. In contrast to the term describing contributions from thermal and quantum fluctuations the sign of the constant A' is positive, i.e. the static fluctuations stabilize the most uncollinear phases

with sublattice moments inclined at an angle close to 90°. The absolute values of A and A' increase with increasing temperature and concentration of defects, respectively. The competition of these two mechanisms predetermines the magnetic phase diagram to differ essentially from that of TLAF without defects. In the fields near $H_{sat}/3$ starting from a certain threshold level of doping the fan phase shown schematically in Fig. 1(b) is expected at low temperatures. The fan phase can be replaced by the uud phase at higher temperatures where the biquadratic exchange term with the negative sign dominates.

The second report (Ref. [12]) shows that $Rb_{1-x}K_xFe(MoO_4)_2$ is an example of a system with competing thermal and static fluctuations. It was found that in the low field range and at low temperatures the ESR spectra change drastically with K doping. The observed spectra in the doped samples were explained by the transition from the Y phase to the fan phase as the doping increases. The magnetization curves $M(H)$ of $Rb_{1-x}K_xFe(MoO_4)_2$ were studied for samples with $x = 0, 0.025, 0.075$, and 0.15. The suppression of magnetization plateau was observed with K doping at fields near $H_{sat}/3$ at low temperatures. The plateau characteristic of the uud phase is more noticeable at higher temperatures. This tendency was ascribed to the restoration of the uud phase by thermal fluctuations in a high temperature region.

We report ^{87}Rb NMR study of $Rb_{1-x}K_xFe(MoO_4)_2$ to obtain information about the magnetic structure at fields near $H_{sat}/3$, which is expected to be strongly perturbed with an increase of doping.

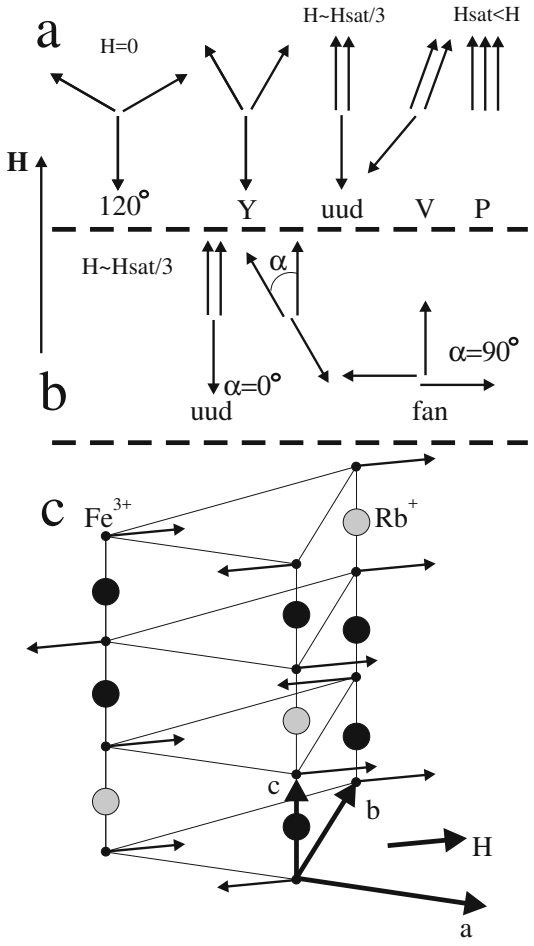

FIG. 1: (color online) (a) Magnetic structures expected for the XY TLAF with an in-plane external field as the field increases. (b) Magnetic structures with the total magnetization $M = M_{sat}/3$. (c) Crystal structure of $RbFe(MoO_4)_2$. The small circles are the positions of Fe^{3+} magnetic ions, the bigger circles (both black and gray, see text) are the positions of Rb^+ ions, the $(MoO_4)^{2-}$complexes are not shown. One magnetic cell of the uud phase is shown. $\mathbf{a}, \mathbf{b}$, and $\mathbf{c}$ are the basis vectors describing the crystallographic structure, $\mathbf{a}, \mathbf{b}$ are directed along the sides of the triangle while $\mathbf{c}$ is aligned along $\mathbf{C}^3$. The translational vectors of the uud structure are $\mathbf{a}+2\mathbf{b}$ and $2\mathbf{a}+\mathbf{b}$. The short arrows depict the expected orientations of magnetic moments in the uud phase with a period of $3c$ for the direction of the magnetic field $\mathbf{H}$ as shown.

II. CRYSTAL AND MAGNETIC STRUCTURE

The crystal structure of $RbFe(MoO_4)_2$ consists of alternating layers of Fe^{3+}, $(MoO_4)^{2-}$ and Rb^+ ions situated perpendicularly to the threefold axis C^3. Inside the layers, the ions form regular triangular lattices. Fig. 1(c) shows the magnetic Fe^{3+} ions ($5d^3$, $S = 5/2$) and the non-magnetic Rb^+ ions, the $(MoO_4)^{2-}$ complexes are not shown.[13] The crystal structure at room temperature belongs to space group $P\bar{3}m1$ and below 190 K is lowered to space group $P\bar{3}c1$.[14] The magnetic ordering occurs at $T_N \approx 3.8$ K.[2] At fields near $H_{sat}/3$ the commensurate uud magnetic structure with the propagation vector $(1/3, 1/3, 1/3)$ is established,[1–5] Fig. 1(b). The magnetic cell of this structure contains 9 formula units. The six Rb^+ ions shown in black are located in equivalent magnetic environment with two neighboring Fe^{3+} ions with oppositely directed spins. The other three gray-colored Rb^+ ions are sandwiched between neighboring Fe^{3+} moments that have parallel orientation. For this magnetic structure two NMR lines with the intensity ratio 2 : 1 are expected. Such NMR spectra were observed experimentally and successfully modeled in Ref. [15].

In the present work K doped $RbFe(MoO_4)_2$ was studied. The K^+ ionic radius is close to the ionic radius of Rb^+. The crystal growth technique is discussed in Refs. [2,12]. The charge and radius matching of these ions guarantees that K^+ ions replace the Rb^+ ions in the doped samples. The temperature of the transition from paramagnetic to magnetically ordered state monotonically decreases from 4 K ($x = 0$) to ≈ 2.8 K ($x = 0.15$) together with the values of H_{sat} from 18.6 T ($x = 0$) to 16.7 T ($x = 0.15$).[12] For each x the transition was identified by a sharp anomaly on the temperature dependence of the magnetic susceptibility. This fact allows us to believe that at these K concentrations the K^+ ions are uniformly distributed in Rb matrix, and

$Rb_{1-x}K_xFe(MoO_4)_2$ is an excellent system for experimental study of TLAF with static random deviations of exchange bonds. According to theoretical predictions at high doping level the *fan* structure shown in Fig. 1(b) is expected. This phase can be obtained by rotation of two antiparallel spins of the *uud* phase by an angle of $\alpha = \pi/2$. If the propagation vector of the *fan* structure is the same as for the *uud* structure in undoped samples, the two peak NMR spectrum is expected with the intensity ratio 2 : 1. In contrast to the *uud* phase the more intense line corresponds to the NMR signals from Rb^+ ions which have two neighbor Fe^{3+} spins, one directed along the magnetic field and the second is perpendicular to the magnetic field. The second line corresponds to the NMR signal from the Rb^+ ions with two nearest neighbor spins which are perpendicular to the magnetic field. The premise of this study is that the effective fields from the neighbor magnetic ions on the Rb nuclei for the *fan* phase essentially differ in comparison with the *uud* phase which should be reflected in ^{87}Rb NMR spectra.

III. SAMPLE PREPARATION AND EXPERIMENTAL DETAILS

The samples used in the experiments were from the same batch as in Ref. [12]. The x-ray study showed that all samples were single-phased.[12] The typical size of the crystal was $2 \times 2 \times 0.5$ mm^3 with the smallest dimension corresponding to the C^3 direction of the crystal. NMR measurements were taken in a superconducting 9 T magnet and a superconducting Cryomagnetics 17.5 T magnet at the Augsburg University and the National High Magnetic Field Laboratory, respectively. ^{87}Rb nuclei (nuclear spin $I = 3/2$, gyromagnetic ratio $\gamma/2\pi = 13.9318$ MHz/T) were probed using pulsed NMR technique. The spectra were obtained by summing fast Fourier transforms (FFT) or integrating the averaged spin-echo signals as the field was swept through the resonance line. Utilizing FFT techniques, NMR spin echoes were obtained using $\tau_p - \tau_D - 2\tau_p$ pulse sequences, where the pulse lengths τ_p were 1 μs and the times between pulses τ_D were 15 μs. The spectra with integrated spin-echo signals were collected by pulse sequences with $\tau_p = 4$ μs and $\tau_D = 12$ μs. T_1 was extracted using a multiexponential expression which is utilized in spin-lattice relaxation when NMR lines are split by quadrupole interaction.[16]

Measurements were carried out in the temperature range $1.43 \leq T \leq 25$ K stabilized with a precision better than 0.1 K.

IV. EXPERIMENTAL RESULTS

Fig. 2 shows ^{87}Rb NMR spectra measured in the samples with different K doping in the ordered and paramagnetic states at applied magnetic fields close to $H_{sat}/3$.

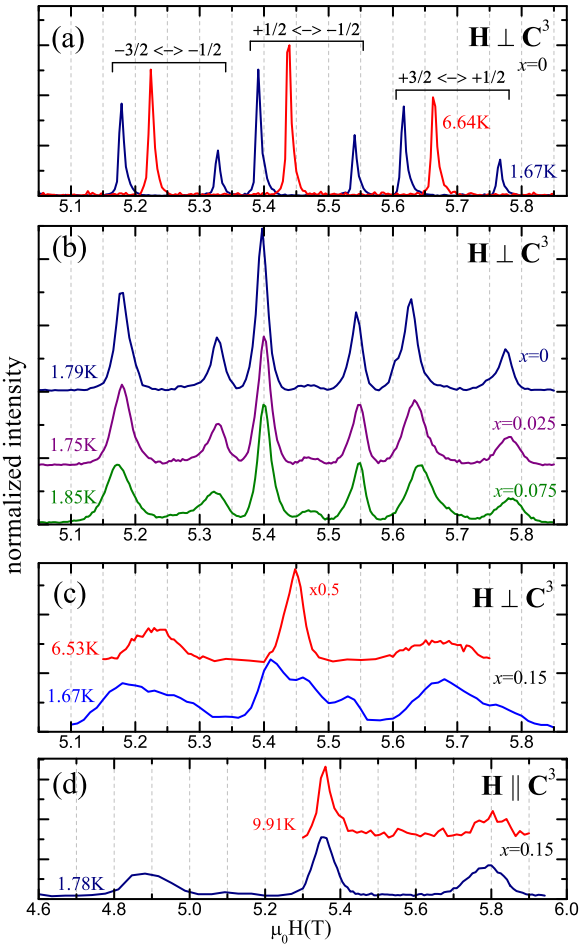

FIG. 2: (color online) ^{87}Rb NMR spectra of $Rb_{1-x}K_xFe(MoO_4)_2$, $\nu = 75.5$ MHz, (a),(b),(c) $\mathbf{H} \perp \mathbf{C}^3$, (d) $\mathbf{H} \parallel \mathbf{C}^3$.

The spectra in Fig. 2(a) are taken from Ref. [15]. In the paramagnetic state all Rb^+ ions are in equivalent positions and the spectrum consists of three lines: the central line corresponds to the transition ($m_I = -1/2 \leftrightarrow +1/2$) and two quadrupole split satellites correspond to the transitions ($m_I = \pm 3/2 \leftrightarrow \pm 1/2$). For $x = 0, 0.025$, and 0.075 below the magnetic ordering temperature, each single line splits into two with the low-field line two times more intense than the high-field one. The two lines corresponding to $(-1/2 \leftrightarrow +1/2)$ transition look similar, whereas the satellite lines demonstrate an increase of non-uniform quadrupolar broadening with an increase of K doping. This is because the first order broadening is zero for the central transition in contrast to the satellites. The shape of the spectra for such small dopings is well described by the *uud* structure.[15]

The spectrum for $x = 0.15$ in the ordered state looks different, Fig. 2(c). The central line has a fine structure revealing non-equivalence of Rb positions. The same structure is smeared for the satellites due to quadrupolar broadening which can also be observed in the correspond-

ing spectra in the paramagnetic state.

Fig. 2(d) shows the spectra for $x = 0.15$ and $\mathbf{H} \parallel \mathbf{C}^3$. The spectrum in the ordered state consists of single lines as in the paramagnetic state. This means that the magnetic structure of K-doped samples lies within triangular plane as in pure samples ($x = 0$).[15] The satellites are essentially broader than the central line due to quadrupolar broadening arising from K doping.

The spectra shown in Figs. 2(b), 2(c), and 2(d) were measured on samples that consists of 4-5 single crystals glued together in such a way that their C^3 axis coincide. The single crystal and the composite samples spectra were similar except the linewidth for $(-1/2 \leftrightarrow +1/2)$ transition: the line in the composite samples were approximately twice as wide as in the single crystals. We attribute this to the demagnetization fields from the neighbor crystals in the composite sample. So the broadening of the central line is mostly defined by the demagnetization fields, whereas the broadening of the satellites is due to nonuniformity of quadrupolar interactions. Next we will discuss in detail the magnetic structure of the sample with $x = 0.15$. To minimize broadening a single crystal was used and the fine structure of the line corresponding to the central transition only was analysed.

The temperature evolution of ^{87}Rb NMR spectra obtained by FFT technique at $1.43 < T < 25$ K is shown in Fig. 3. The frequency 81 MHz corresponds to resonance fields, where the applied magnetic field is close to $H_{sat}/3$. Note here that in all doped samples we measured ^{87}Rb NMR spectra at fields corresponding to the magnetization plateau in Ref. [12]. The field evolution of ^{87}Rb NMR spectra at $T \approx 1.47$ K, shown in Fig. 4, was measured up to $\mu_0 H \approx 17$ T which exceeds the saturation field ($\mu_0 H_{sat} \approx 14$ T). The spectra in the paramagnetic state are shown with green lines, the spectra in the ordered state are shown with blue lines. The field and temperature of the transition from paramagnetic to magnetoordered state (H_c, T_c) were found from sharp λ-like anomalies in the field and temperature dependences of the ^{87}Rb spin lattice relaxation rate T_1^{-1} shown in Fig. 5. The obtained T_c and H_c well coincide with those values determined from differential susceptibility measurements in samples with the same K doping.[12]

Within the paramagnetic phase ($T > T_c$ or $H > H_c$) ^{87}Rb NMR spectra consists of two lines with intensity ratio close to 1 : 4. The simplest way to explain the presence of two lines with such intensity ratio is to attribute the more intense line to Rb nuclei which have two nearest Rb^+ ions located above and below in C^3 direction while the weaker line belongs to Rb nuclei joined to K^+ ions.[17] This also explains the small difference in the positions of two lines. The spectral shift of each line is proportional to the value of Fe^{3+} magnetic moment. As a result the distance between two lines in the saturated phase is approximately three times greater than in the fields near $H_{sat}/3$ in the paramagnetic phase.[18]

The NMR lines in Fig. 3 broaden as the temperature is decreased and at temperatures below 7 K the two lines become unresolvable. At temperatures below T_c the fine structure appears and the spectra take the form of three broad maxima which is sharply different from the two-lines spectra pattern characteristic of the *uud* phase and observed in the samples with smaller K dopings (see Fig. 2(b)).

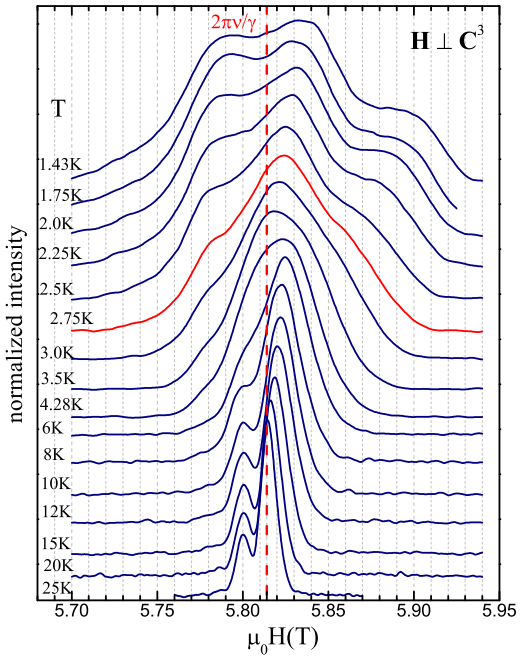

FIG. 3: (color online) Temperature evolution of ^{87}Rb NMR spectra ($m_I = +1/2 \leftrightarrow -1/2$ transition) in $Rb_{0.85}K_{0.15}Fe(MoO_4)_2$, $\nu = 81$ MHz, $\mathbf{H} \perp \mathbf{C}^3$. The spectrum shown with red line corresponds to the maximum of ^{87}Rb spin lattice relaxation rate T_1^{-1} shown in Fig. 5(a).

Fig. 4 shows that except for magnetic broadening, the shape of the spectra in the saturated phase ($H > H_c$) is very similar to that of the spectra in the paramagnetic phase at low fields. The field distance between the two lines and their widths increase as the field is increased showing that these values are proportional to the magnetization of the sample. So the presence of two lines can be explained by the distribution of the effective fields from neighboring magnetic ions arising from random K substitution. In the next section we will discuss the possible magnetic structures which can describe the observed NMR spectral shapes in the ordered state.

V. DISCUSSION

Theoretical study of magnetic structures of TLAF in 2D model leads to three sublattice structures with propagation vector (1/3,1/3). If one considers Zeeman and exchange energies only, the structures with the same net magnetic moment have nearby energy values. The magnetic structure realized is determined by taking into account the energies of thermal and quantum fluctuations.

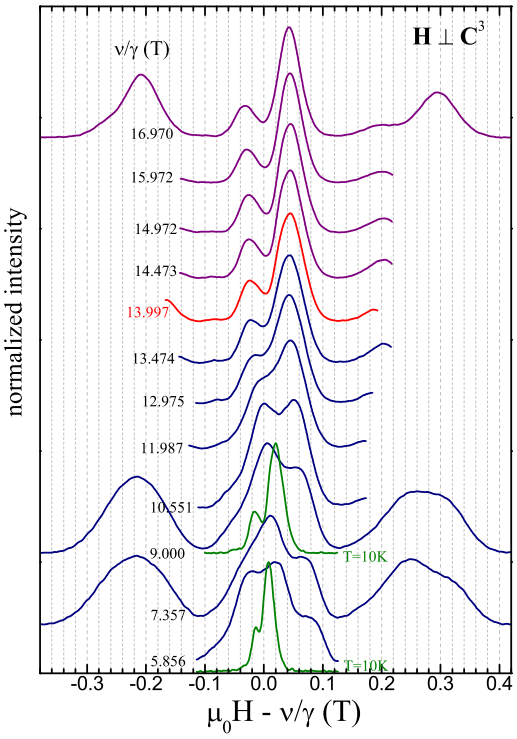

FIG. 4: (color online) Field evolution of ^{87}Rb NMR spectra in $Rb_{0.85}K_{0.15}Fe(MoO_4)_2$ at temperature ≈ 1.47 K, $\mathbf{H} \perp \mathbf{C}^3$. The spectrum shown with red line corresponds to the maximum of ^{87}Rb spin lattice relaxation rate T_1^{-1} shown in Fig. 5(b). The green colored spectra correspond to paramagnetic state ($T = 10$ K).

At the fields close to $H_{sat}/3$ the *uud* phase is energetically preferable. A set of structures with $M = M_{sat}/3$ can be designed as in Fig. 1(b), where α determines a specific structure, e.g., $\alpha = 0°$ for the *uud* structure.

In case of real 3D TLAF the choice of magnetic structure in triangular planes is defined not only by fluctuations, but also by any small interactions of exchange and relativistic nature. According to neutron diffraction experiments[5] at low and high field ranges ($0 < \mu_0 H <$ 3.2 T and 9.5 T $< \mu_0 H < \mu_0 H_{sat}$) the magnetic structure of $RbFe(MoO_4)_2$ is incommensurate with propagation vector $(1/3, 1/3, k_{ic})$. In this case an individual magnetic structure from a set of nearly degenerate magnetic structures with the same net magnetic moment is realized in each triangular plane. The incommensurate harmonic alternation of these magnetic structures along the C^3 axis is defined by the dominant interplane interactions in these disjunct field ranges.[19]

For the intermediate field range (3.2 T $\leq \mu_0 H \leq$ 9.5 T) fluctuations are dominant and in each triangular plane identical magnetic structures are established. With increasing field, they evolve in a sequence expected for a single triangular plane, i.e. the Y, *uud*, and V phases, (see Fig. 1(a)).

^{87}Rb NMR spectra in $Rb_{1-x}K_xFe(MoO_4)_2$, $x = 0, 0.025$, and 0.075, can be well described by the model of the *uud* magnetic structure using the values of quadrupole constants obtained in Ref. [15] with the value of Fe^{3+} magnetic moment as the only fitting parameter. The main contribution to the effective magnetic field at the Rb nuclei is produced by the dipolar fields from the neighboring magnetic ions and partly by the contact Fermi field from two adjacent magnetic Fe^{3+} ions above and below the Rb ion. The contact field constant $A = 2.5$ mT$/\mu_B$ was obtained from the spectral shift in the paramagnetic phase. The results of modeling with the magnetic moment of 5 μ_B is shown in Fig. 6(e). The values of the magnetic moments for the samples with $x = 0$ and $x = 0.025, 0.075$ were the same. A difference of 8 % between the values of the magnetically ordered moment found in this work and our previous work[15] is due to taking into account the contact field in the present spectra simulations. Here we must emphasize that for the particular case of magnetic structures with propagation vector (1/3,1/3) within triangular plane the shape of ^{87}Rb NMR spectra is sensitive only to the component of the magnetic moment which is parallel to the magnetic field. This statement can be proved analytically. It means that the two peak spectra with specific 2 : 1 intensity ratio are consistent with each of the structures Y, *uud*, and V with commensurate interplane ordering.

Note, that the value of the Fe^{3+} magnetic moment does not depend on the doping, whereas the field dependence of the magnetization near $H_{sat}/3$ changes drastically. The sample with $x = 0$ demonstrates the plateau in the $M(H)$ dependence in this field range, whereas the doped samples demonstrate only a weak deviation of $M(H)$ from linear dependence, which can be seen only in the field dependencies of differential susceptibility.[12] The linear dependence of $M(H)$ is expected for the quasiclassical behavior with realization of the *uud* phase exactly at $H_{sat}/3$ as a boundary point between Y and V phases.

The shapes of ^{87}Rb NMR spectra for $x = 0.15$ drastically differ from those for $x = 0, 0.025$, and 0.075, showing changes in the magnetic structure. According to temperature dependences of the magnetization[12] and spin-lattice relaxation rate in Fig. 5, there is a sharp transition into an ordered state at $T_c \approx 2.8$ K which allows us to expect a single-phase magnetic state at low temperature. As mentioned earlier, the data for $x = 0.15$ and $\mathbf{H} \parallel \mathbf{C}^3$, Fig. 2(d), imply that magnetic structures with the spins within triangular planes should be considered. Following the suggestions of the theory in Ref. [10] for the 2D case we simulated[20] the spectra for the *uud* ($\alpha = 0°$) and the *fan* ($\alpha = 90°$) structures within the triangular planes. First we consider the structures that were stacked up in the C^3 direction with periodicity $2c$ and $3c$. The results are shown in Figs. 6(a) and 6(b). The simulated spectra consist of two lines with intensity ratio 2 : 1 and 1 : 2. Such spectra shapes were not observed experimentally for $x = 0.15$. Next we consider the model of 2D ordered triangular magnetic planes with propagation vector (1/3,1/3), i.e. with interplane disorder, Figs. 6(c)

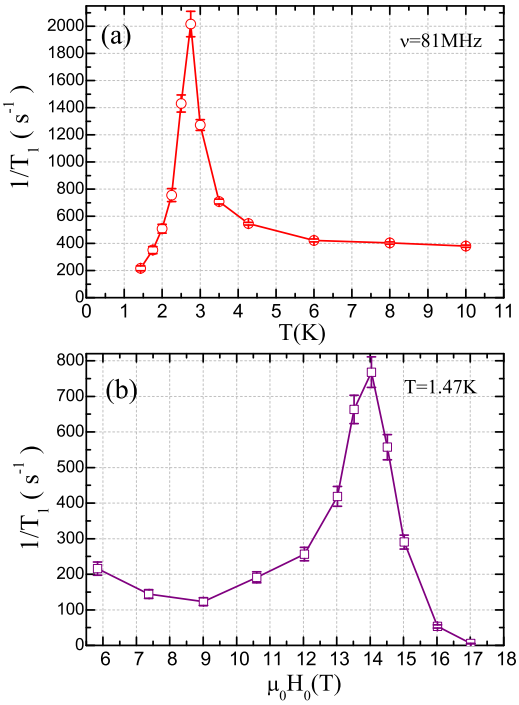

FIG. 5: (color online) (a) Temperature dependence of ^{87}Rb spin lattice relaxation rate T_1^{-1} in $Rb_{0.85}K_{0.15}Fe(MoO_4)_2$ at field 5.82 T, $\mathbf{H} \perp \mathbf{C}^3$. (b) Field dependence of ^{87}Rb spin lattice relaxation rate T_1^{-1} in $Rb_{0.85}K_{0.15}Fe(MoO_4)_2$ at temperature 1.47 K, $\mathbf{H} \perp \mathbf{C}^3$.

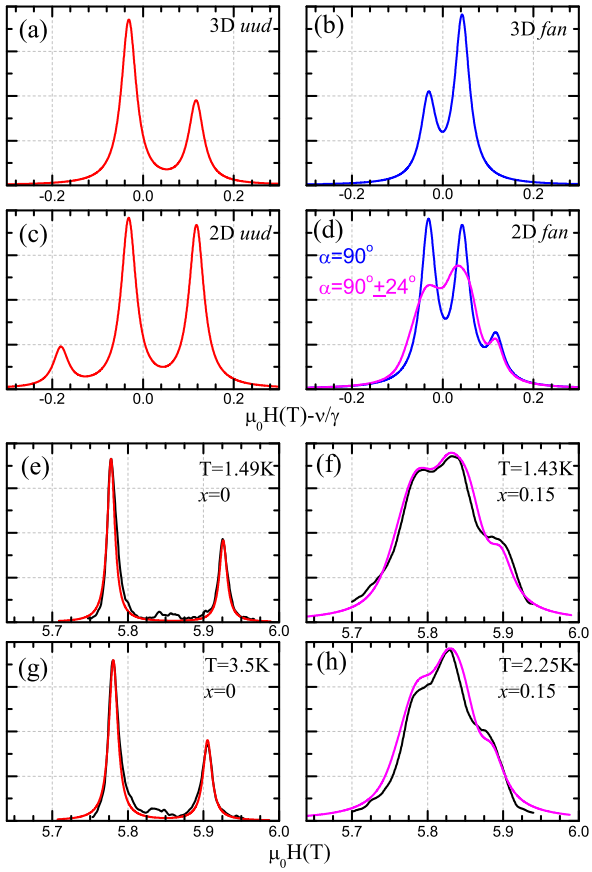

FIG. 6: (color online) Simulated NMR spectra corresponding to the *uud* structure ($\alpha = 0°$, left panels) and the *fan* structure ($\alpha = 90°$, right panels), $\mathbf{H} \perp \mathbf{C}^3$. For comparison experimental ^{87}Rb NMR spectra (black lines) at frequency 81 MHz, $\mathbf{H} \perp \mathbf{C}^3$, and two temperatures are shown for (e),(g) $x = 0$ and (h),(f) $x = 0.15$. Simulated spectra data: (a) 3D *uud* with periodicity $2c$ or $3c$ in the C^3 direction, $\mu = 5\mu_B$, individual linewidth $\delta = 20$ mT; (b) 3D *fan* with periodicity $2c$ or $3c$ in the C^3 direction, $\mu = 5\mu_B$, $\delta = 20$ mT; (c) 2D *uud*, $\mu = 5\mu_B$, $\delta = 20$ mT; (d) 2D *fan*, $\mu = 5\mu_B$, $\alpha = 90°$ (blue line), $\alpha = 90° \pm 24°$ (magenta line), $\delta = 20$ mT; (e) 3D *uud*, $\mu = 5\mu_B$, $\delta = 6$ mT; (f) 2D *fan*, $\mu = 3.7\mu_B$, $\alpha = 90° \pm 24°$, $\delta = 20$ mT; (g) 3D *uud*, $\mu = 4.2\mu_B$, $\delta = 7$ mT; (h) 2D *fan*, $\mu = 3.3\mu_B$, $\alpha = 90° \pm 22°$, $\delta = 20$ mT.

and 6(d). These models describe the main feature of the observed spectra – the shape with three maxima. The intensity ratios are $1:4:4$ and $4:4:1$. For $\alpha = 0°$ (the Y, *uud*, and V structures) the low intensity line is expected at lower field, whereas for $\alpha = 90°$ (the *fan*-structure) the low intensity line is expected at higher field. The low intensity line corresponds to NMR signals from Rb nuclei situated between the ferromagnetically ordered planes. Such line is absent for 3D magnetically ordered commensurate structure with dominant antiferromagnetic interplane interaction. The suggestion about interplane disorder for K doped samples seems to be natural because the interplane interaction is small. The loss of interplane ordering due to defects was earlier observed in other planar spiral structures $LiCu_2O_2$,[21] $LiCuVO_4$,[22] and $CuCrO_2$.[23] The intensity ratio between the lines of the experimental spectra corresponds to the simulated spectrum of the *fan*-structure, Fig. 6(d). The best agreement with the experiment can be obtained if one assumes the distribution of α within a certain range of angles centered at 90°, and α is randomly selected within this range for each triangular plane. Figs. 6(e),6(g) and Figs. 6(f),6(h) show the result of simulations at two temperatures for $x = 0$ and $x = 0.15$, respectively. The fitting parameters for the low temperature spectra are $\alpha = 0°$, $\mu = 5\mu_B$ for $x = 0$ (Fig. 6(e)) and $\alpha = 90° \pm 24°$, $\mu = 3.7\mu_B$ for $x = 0.15$ (Fig. 6(f)). At higher temperatures the simulation gives a smaller value of the magnetic moment. The theoretically predicted transition from the *fan* phase to the *uud* phase as the temperature increases was not observed in our NMR experiments for $x = 0.15$. Finally note that NMR probes local fields and as a result is sensitive to short range static correlations only.

VI. CONCLUSIONS

^{87}Rb NMR spectra in $Rb_{1-x}K_xFe(MoO_4)_2$ with $x = 0, 0.025$, and 0.075 below the ordering temperature and at the magnetic fields close to $H_{sat}/3$ can be described by the 3D magnetic order with the *uud* like projections on the field direction. The value of the magnetic moment

projected on the field direction is $(5 \pm 0.2)\mu_B$ (close to $gS\mu_B$).

In the samples with $x = 0.15$, our NMR experiments detect the magnetic order at $T_c \approx 2.75$ K, where the shape of ^{87}Rb NMR spectra pattern substantially differs from that in the samples with lower dopings. The observed NMR spectra below T_c can be well described by a 2D fan magnetic structure with three sublattices within each triangular plane. The alternation of three possible configurations of three sublattices for neighboring triangular planes is random. This fan structure describing our NMR data is in agreement with theoretical expectations for the 2D TLAFs with spatially fluctuating exchange parameters.[10]

Acknowledgments

We thank A.I. Smirnov and M.E. Zhitomirskiy for stimulating discussions. Yu.A.S. thanks the Government of the Republic of Tatarstan for the support through Algarysh Grant. The work was supported in part by the Program of the Presidium of RAS 1.4. "Actual problems of low temperature physics". The theoretical and experimental parts of this work were supported by Russian Science Foundation Grant No. 17-02-01505. We gratefully acknowledge support by the German Research Society (DFG) via TRR80 (Augsburg, Munich). Work at the National High Magnetic Field Laboratory is supported by the User Collaborative Grants Program (UCGP) under NSF Cooperative Agreement No. DMR-1157490, and the State of Florida.

* Electronic address: svistov@kapitza.ras.ru

[1] T. Inami, Y. Ajiro, and T. Goto, J. Phys. Soc. Jpn. **65**, 2374 (1996).
[2] L. E. Svistov, A. I. Smirnov, L. A. Prozorova, O. A. Petrenko, L. N. Demianets, and A. Ya. Shapiro, Phys. Rev. B **67**, 094434 (2003).
[3] G. A. Jorge, C. Capan, F. Ronning, M. Jaime, M. Kenzelmann, G. Gasparovic, C. Broholm, A. Ya. Shapiro, L. N. Demianets, Physica B **354**, 297 (2004).
[4] L. E. Svistov, A. I. Smirnov, L. A. Prozorova, O. A. Petrenko, A. Micheler, N. Büttgen, A. Ya. Shapiro, and L. N. Demianets, Phys. Rev. B **74**, 024412 (2006).
[5] M. Kenzelmann, G. Lawes, A. B. Harris, G. Gasparovic, C. Broholm, A. P. Ramirez, G. A. Jorge, M. Jaime, S. Park, Q. Huang, A. Ya. Shapiro, and L. A. Demianets, Phys. Rev. Lett. **98**, 267205 (2007).
[6] A. I. Smirnov, H. Yashiro, S. Kimura, M. Hagiwara, Y. Narumi, K. Kindo, A. Kikkawa, K. Katsumata, A. Ya. Shapiro, and L. N. Demianets, Phys. Rev. B **75**, 134412 (2007).
[7] S. E. Korshunov, J. Phys. C: Solid State Phys. **19**, 5927 (1986).
[8] D. H. Lee, J. D. Joannopoulos, J. W. Negele, D. P. Landau, Phys. Rev. B **33**, 450 (1986).
[9] R. S. Gekht and I. N. Bondarenko, J. Exp. Theor. Phys. **84**, 345 (1997).
[10] V. S. Maryasin and M. E. Zhitomirsky, Phys. Rev. Lett. **111**, 247201 (2013).
[11] M. E. Zhitomirsky, J. Phys. Conf. Ser. **592**, 012110 (2015).
[12] A. I. Smirnov, T. A. Soldatov, O. A. Petrenko, A. Takata, T. Kida, M. Hagiwara, A. Ya. Shapiro, and M. E. Zhitomirsky, Phys. Rev. Lett. **119**, 047204 (2017).
[13] R. F. Klevtsova and P. V. Klevtsov, Kristallografiya **15**, 953 (1970).
[14] S. A. Klimin, M. N. Popova, B. N. Mavrin, P. H. M. van Loosdrecht, L. E. Svistov, A. I. Smirnov, L. A. Prozorova, H.-A. Krug von Nidda, Z. Seidov, A. Loidl, A. Ya. Shapiro, and L. N. Demianets, Phys. Rev. B **68**, 174408 (2003).
[15] L. E. Svistov, L. A. Prozorova, N. Büttgen, A. Ya. Shapiro, and L. N. Demyanets, JETP Lett. **81**, 102 (2005).
[16] A. Suter, M. Mali, J. Roos, and D. Brinkmann, J. Phys.: Condens. Matter **10**, 5977 (1998).
[17] For such a model the observed intensity ratio for a random distribution of K ions corresponds to $x = 0.11 \pm 0.01$. Note here, that a few models can be proposed to explain two different positions of Rb ions in K doped samples, we considered the simplest one, and this question requires a special experimental study.
[18] Note here that the value of Fe^{3+} magnetic moment at 10 K differs from that value at 1.4 K not more than 10 %,[4] this allows us to evaluate the magnetic moment at 10 K as $M(H) \approx M_{sat}/H_{sat} \cdot H$.
[19] J. S. White, Ch. Niedermayer, G. Gasparovic, C. Broholm, J. M. S. Park, A. Ya. Shapiro, L. A. Demianets, and M. Kenzelmann, Phys. Rev. B **88**, 060409(R) (2013).
[20] The program can be found at http://www.kapitza.ras.ru/rgroups/esrgroup/numa.html.
[21] A. A. Bush, N. Büttgen, A. A. Gippius, V. N. Glazkov, W. Kraetschmer, L. A. Prozorova, L. E. Svistov, A. M. Vasiliev, and A. Zheludev, Phys. Rev. B **88**, 104411 (2013).
[22] L. A. Prozorova, S. S. Sosin, L. E. Svistov, N. Büttgen, J. B. Kemper, A. P. Reyes, S. Riggs, A. Prokofiev, and O. A. Petrenko, Phys. Rev. B **91**, 174410 (2015).
[23] T. Okuda, K. Uto, S. Seki, Y. Onose, Y. Tokura, R. Kajimoto, and M. Matsuda, J. Phys. Soc. Jpn. **80**, 014711 (2011).